Chapter 2
Extension of Chatter Theory

2.1 Introduction

In the previous chapter, regenerative chatter theory was developed for turning and in particular for a facing operation. It is appropriate to summarise the assumptions made in the theory that was presented.

- A linear model of the process was assumed; that is, nonlinearities were ignored. It was argued that the onset of chatter will initially involve small amplitudes of vibration, and so, a linear model could reasonably be assumed when investigating the onset of chatter.
- Both the average and oscillating components of the cutting force were assumed to act in the same fixed direction.
- The cutting force was initially assumed to be proportional to the undeformed chip cross-sectional area and not dependent on the cutting speed. Subsequently, an additional force component was added that depended on the penetration rate of the tool into the work and this resulted in process damping.
- Only vibration in the direction that affected chip thickness was considered.
- A graphical method [1] of determining the stability boundary was presented, and the machine response used as an example had a single mode of vibration representing a one-degree-of-freedom system.

There are therefore several questions that need to be raised. Do the assumptions made give rise to any serious errors when solutions to chatter problems are attempted? What about real machine responses that involve multiple modes of vibration rather than a single mode? Does the chatter theory developed in the previous chapter apply to other machining operations? This chapter addresses these questions.

2.2 Multiple Modes of Vibration

Real machines have multiple modes of vibration. Though there may be a predominant mode, so that the machine response can be represented by the response of a single-degree-of-freedom system, this is not always the case. To illustrate the

B. Stone, *Chatter and Machine Tools*, DOI: 10.1007/978-3-319-05236-6_2,

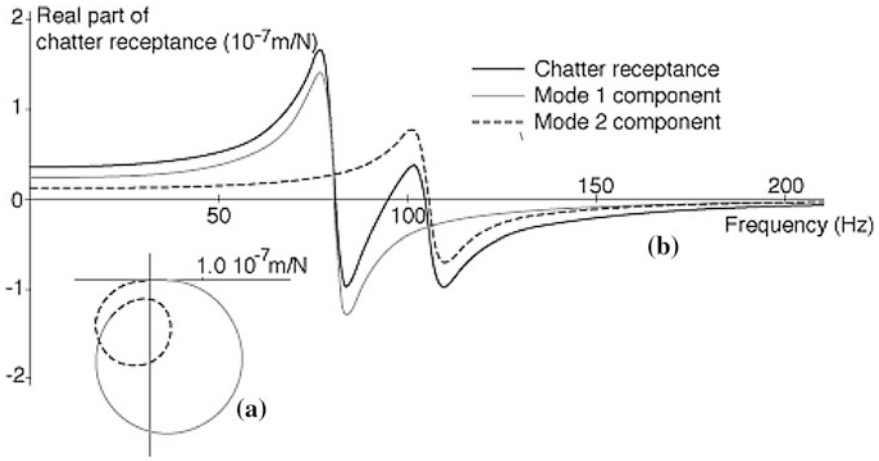

Fig. 2.1 Chatter receptance for a structure with two modes of vibration, **a** chatter receptance and **b** real part (Program 2.1)

effect on chatter of a machine with more than one significant mode, consider a lathe with two modes of vibration. The conventional wisdom is to assume that the response can be represented by the superposition of the responses of two one-degree-of-freedom systems. Thus, the chatter receptance is given by

$$\frac{X_o}{F} = \frac{1}{k_1\left(1 - \frac{\omega^2}{\omega_{n1}^2} + i2\xi_1\frac{\omega}{\omega_{n1}}\right)} + \frac{1}{k_2\left(1 - \frac{\omega^2}{\omega_{n2}^2} + i2\xi_2\frac{\omega}{\omega_{n2}}\right)}$$

Figure 2.1 shows the chatter receptance for some typical values of the mode parameters chosen to give equal values of the maximum negative in-phase component of the chatter receptance at two frequencies.

Mode 1: $k_1 = 4 \times 10^7$ N/m, $\omega_{n1} = 80$ Hz, $\xi_1 = 0.044$
Mode 2: $k_2 = 8 \times 10^7$ N/m, $\omega_{n2} = 105$ Hz, $\xi_2 = 0.04$

The graphical method [1] for predicting the stability chart is readily applied to this chatter receptance. For a facing operation, as considered in the previous chapter, a stability chart as shown in Fig. 2.2 is obtained. This chart does not include the process damping resulting from penetration rate effects. If these are included, the predicted stability chart is as shown in Fig. 2.3. The process damping has a proportionally greater effect on the mode with the higher natural frequency as this mode produces shorter wavelength surface waves for the same rotational speed.

Even at this stage, it is clear that chatter theory involves some complexity and it is to be extended even further in this chapter. To avoid being overwhelmed by the increasing complexity, we will adopt the approach initially developed by Tlusty [2] and simply examine the maximum negative in-phase component of the chatter

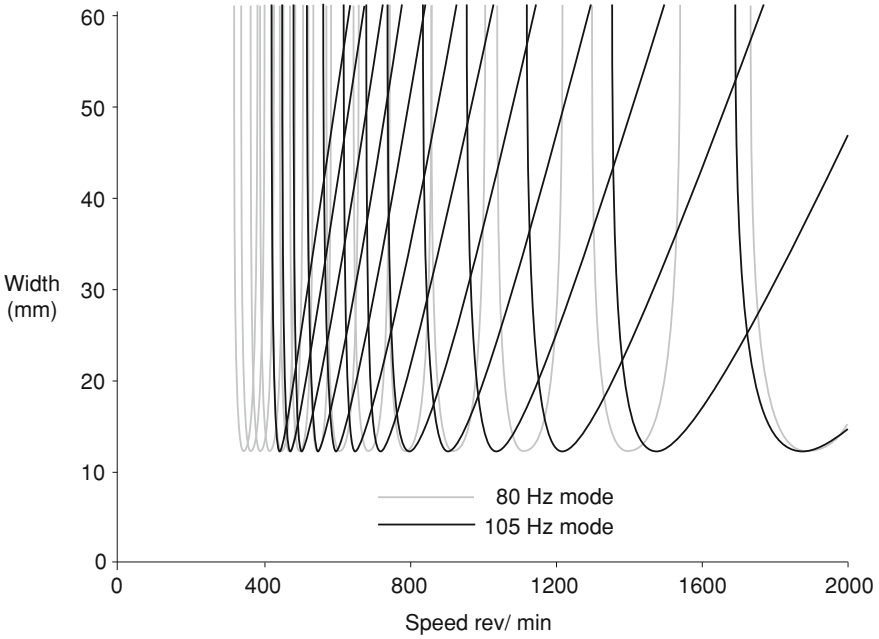

Fig. 2.2 Stability chart with no process damping (Program 2.2)

receptance, knowing that this yields the unconditionally stable (i.e. speed independent) width of cut. In practice, it will be expected that there will be stability lobes and the effects of process damping will give increased stability at lower speeds when there are shorter wavelength surface waves. These effects need to be borne in mind when only the unconditional stable width is calculated.

2.3 Vibration Direction

Thus far, only vibration in the direction that affects chip thickness has been considered. However, in practice, the vibration, resulting from an oscillating cutting force, may occur in a different direction. If the facing operation is reconsidered, then vibration could occur having components in each of the three directions shown in Fig. 2.4 (x, y, z).

Regenerative chatter occurs when a vibration causes a surface wave to be left that one revolution later causes a variation in the cutting force that in turn maintains the vibration or causes it to increase in amplitude. If the vibration is in the x direction as shown in Fig. 2.5a (and as considered in the previous chapter), then such a surface wave is left. However, suppose the vibration was in the z direction, the direction that would change the width of cut as shown in Fig. 2.5b. Any surface wave left on the faced surface will not regenerate one revolution later

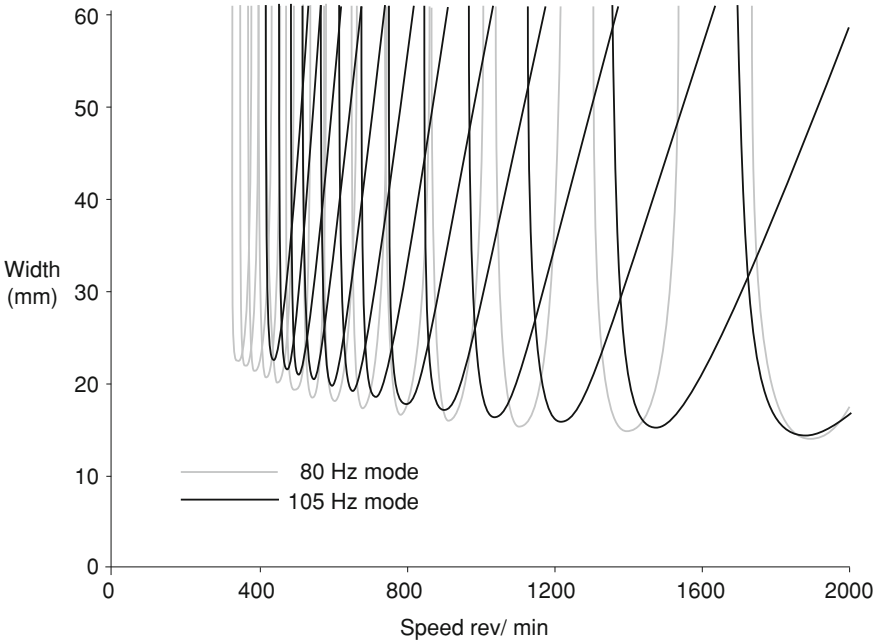

Fig. 2.3 Stability chart with process damping (Program 2.3)

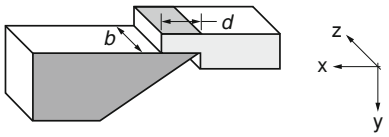

Fig. 2.4 Principal directions of vibration when facing

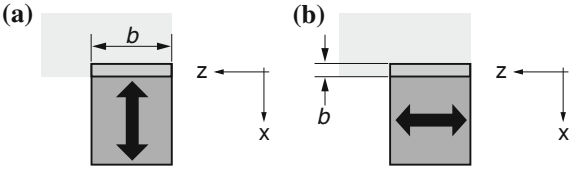

Fig. 2.5 Effective width of cut for vibration in different directions

as the tool has moved in the x direction. However, even if such a wave did regenerate, because the width of cut b will normally be much greater than the depth of cut d, the variation in chip cross-sectional area would be an order of magnitude less than for vibration in the x direction with the same amplitude of vibration. For vibration in the x direction, we have shown that the cutting force F is given by

$F = Rbd = Rb[h - x(t) + x(t - \tau)]$ with an oscillating component $Rb[-x(t) + x(t - \tau)]$

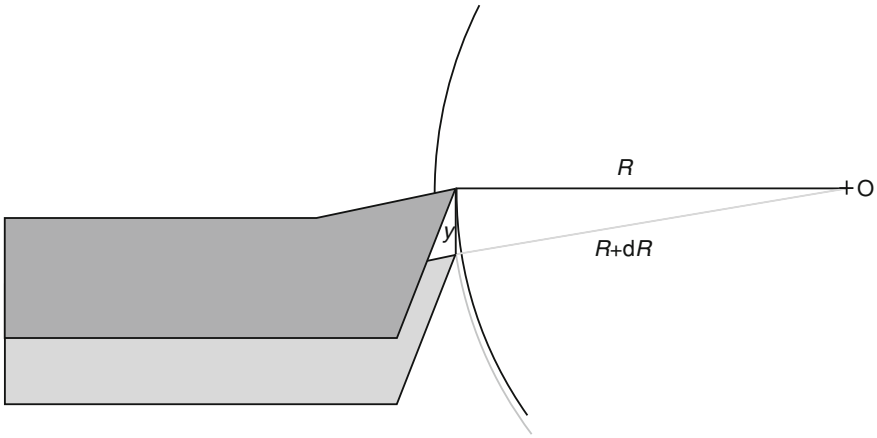

Fig. 2.6 Change in cutting radius for displacement in the y direction

For vibration in the z direction, the equivalent equation would be

$F = Rbd = Rd[b_{\text{mean}} - z(t) + z(t-\tau)]$ with an oscillating component $Rd[-z(t) + z(t-\tau)]$

For identical amplitudes of vibration, i.e. $x(t) = z(t)$, the ratio of the oscillating forces is

$$\frac{F_{x\text{vibration}}}{F_{z\text{vibration}}} = \frac{Rb[-x(t) + x(t-\tau)]}{Rd[-z(t) + z(t-\tau)]} = \frac{b}{d}$$

So that vibration in the z direction causes a far smaller variation in the force, and hence, the prospect of regeneration occurring is greatly reduced.

Now, consider vibration in the y direction (the direction that would cause a change in the cutting speed). This may cause Arnold type B chatter under some circumstances but for the model presented thus far, not regenerative chatter. The amplitude of the wave left on the machined surface is extremely small compared to the amplitude of vibration. For example, if the cutting tool moves down a distance y, then the cutting radius (R) increases to ($R + dR$) and the depth of cut (see Fig. 2.6) is decreased by an amount dR given by

$$(R + dR)^2 = R^2 + y^2 \text{ so that } R^2 + 2RdR + dR^2 = R^2 + y^2$$

And since dR^2 is negligible $dR = y^2/2R = y \cdot y/2R$ and as $y/2R$ is very small, dR is much smaller than y. Hence, the regenerating wave resulting from a vibration in the y direction has a very small amplitude compared to the vibration amplitude, and therefore, the prospect of regeneration occurring is very unlikely.

In practice, any mode of vibration of a machine tool has an associated mode shape and this defines the direction in which the vibration will occur. It is thus

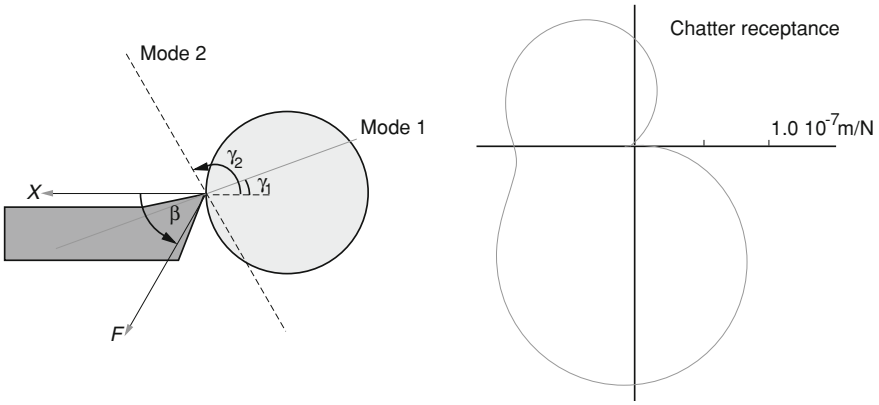

Fig. 2.7 Inclination of mode direction

possible for the mode direction to be, for example, in the x–y plane of Fig. 2.4 and at some angle to the x direction. The effect of the mode direction needs to be considered as it has significant practical application for improving chatter performance.

2.4 Mode Direction

Consider the facing operation with the structural response represented by a single mode that has a mode direction inclined at an angle γ to the horizontal x-axis as shown in Fig. 2.7. Note that X represents the component of the relative displacement between the work and cutting edge, and though F is shown only applied to the cutting edge, there is an equal and opposite force on the work.

The direction of the cutting force F relative to the x direction is β. Let the mode have a direct response (i.e. displacement and force in the mode direction) defined by stiffness k, modal mass m and viscous damping c. The direct response, where both force and displacement are in the mode direction, as shown in Appendix A.6, is given by

$$\frac{X_{\text{direct}}}{F_{\text{direct}}} = \frac{1}{k - m\omega^2 + i\omega c} \tag{2.1}$$

The chatter receptance is the response in the x direction divided by the force (F) in the cutting force direction. The component of F in the mode direction is $F_{\text{direct}} = F\cos(\gamma - \beta)$. The response in the x direction is $X_{\text{direct}} = X/\cos\gamma$. Substituting in Eq. 2.1 gives

$$\frac{X_{\text{direct}}}{F_{\text{direct}}} = \frac{X}{\cos\gamma F\cos(\gamma - \beta)} = \frac{1}{k - m\omega^2 + i\omega c}$$

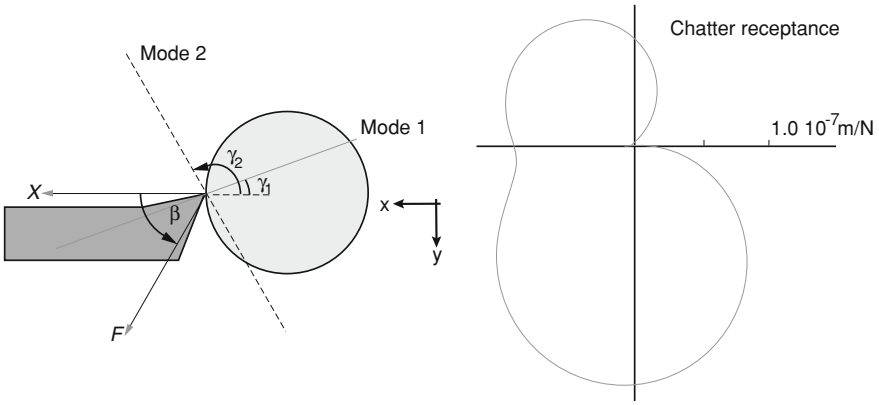

Fig. 2.8 Chatter receptance for a machine with two inclined modes (Program 2.4)

so that the chatter receptance is given by

$$\frac{X}{F} = \frac{\cos\gamma\cos(\gamma-\beta)}{k - m\omega^2 + i\omega c} \tag{2.2}$$

If either $\cos\gamma$ or $\cos(\gamma-\beta)$ is zero, the chatter receptance becomes zero and regenerative chatter will not occur. This is the case when the mode direction is perpendicular to either the x direction (the chip thickness direction) or the cutting force direction.

In practice, the machine response involves several modes, and each has its associated mode direction. In general, when the x direction or cutting force direction is perpendicular to one mode, it will not be so for all the other modes. Thus, the resultant chatter receptance will not be zero. As an example, consider a machine response that has two modes, each of which can be represented by the response of a single-degree-of-freedom system with stiffness k, undamped natural frequency ω_n and damping ratio ξ. Figure 2.8 shows the chatter receptance for a machine with two modes with the following characteristics:

Mode 1: $k_1 = 4 \times 10^7$ N/m, $\omega_{n1} = 100$ Hz, $\xi_1 = 0.05$, mode direction $\gamma = 20^o$
Mode 2: $k_2 = 6 \times 10^7$ N/m, $\omega_{n2} = 120$ Hz, $\xi_2 = 0.02$, mode direction $\gamma = 120^o$

The cutting force direction (β) was assumed to be at 60° to the horizontal x direction. Thus, neither of the modes is perpendicular to the x or F directions and both contribute to the chatter receptance.

The stability chart has stability lobes, but when considering improvements to chatter performance, the unconditional width of cut serves as a suitable indicator. In this example, using a cutting force coefficient of $R = 4.0 \times 10^8$ N/m^2, the unconditional width of cut is 12 mm for the chatter receptance shown.

If on resolving X and F into any mode direction they lie in opposite directions, then the effective mode stiffness (k) is negative. Figure 2.8 illustrates this

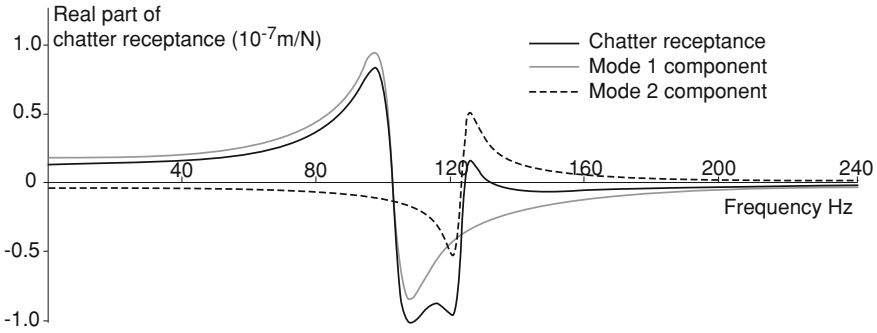

Fig. 2.9 Real part of the chatter receptance showing a negative mode (Program 2.5)

significant feature—it is possible for the chatter receptance to include such a negative mode. This is more clearly seen if the real part of the chatter receptance is plotted against frequency (see Fig. 2.9) and the modal contributions examined. If Mode 2 in Fig. 2.9 was the only mode present, the mean cutting force would cause the tool to move into the work.

Tlusty [2] used negative modes to cancel positive ones and investigated changing the circumferential position of the tool relative to the work for a turning operation. For the mode characteristics and directions used for Fig. 2.8, the tool position may be changed and the unconditional width found. Figure 2.10 shows the variation of the unconditional width of cut with tool position. For the example shown, the conventional tool position has an unconditional width of cut of 12 mm. However, this width would be increased to 45 mm if the tool were positioned at an angle 34° above the horizontal. In the worst position (almost vertically under or over the work), the width is 9 mm. Tlusty [2] measured similar variations experimentally.

Changing the tool position to advantage was noted in the previous chapter. During the discussion of Arnold's [3] paper

> Mr. Alfred Harrison, A.I.Mech.E., commenting on Mr. Pamacott's remarks, said he had found that a great improvement could be achieved by down-cutting, either by putting the tool on the opposite side of the slide or by reversing the direction of the lathe and inverting the tool.

It can be shown that inverting the tool and reversing the rotation may also be advantageous confirming what was known experimentally in 1946. Figure 2.11 shows the variation of unconditional width of cut with position for both an inverted tool and the standard configuration. The mode characteristics listed below have been chosen to show this:

Mode 1: $k_1 = 4 \times 10^7$ N/m, $\omega_{n1} = 100$ Hz, $\xi_1 = 0.05$, mode direction $\gamma = 20^o$
Mode 2: $k_2 = 6 \times 10^7$ N/m, $\omega_{n2} = 140$ Hz, $\xi_2 = 0.02$, mode direction $\gamma = 100^o$

The cutting force direction (β) was again assumed to be at 60° to the x direction.

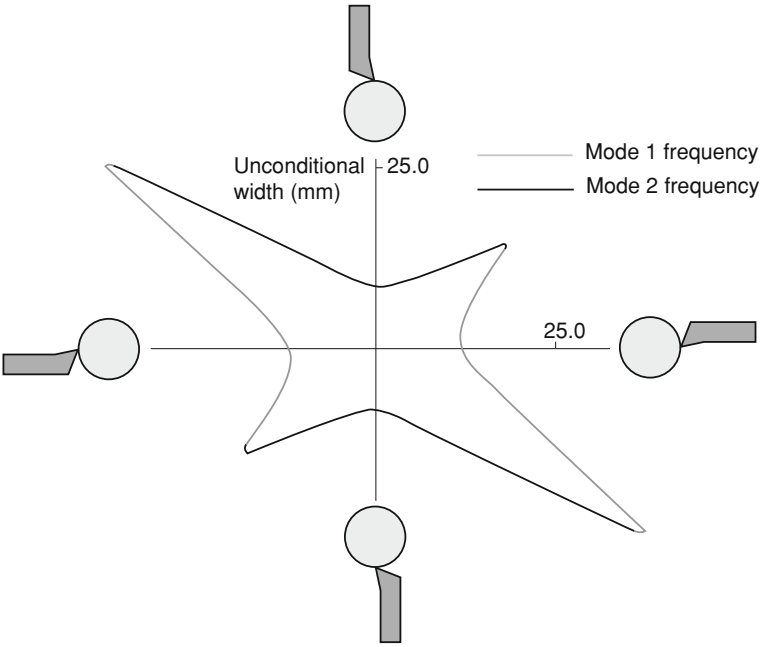

Fig. 2.10 Variation of unconditional width with circumferential position of the tool (Program 2.6)

For the inverted tool in the conventional location (with reverse rotation), the unconditional width is 30 mm, whereas for the not inverted, the width is 13 mm. The total variation of unconditional width with tool position varies between 9 and 45 mm as before.

2.5 Turning, Boring, Drilling and Milling

Thus far, only the specific turning operation of facing has been considered. It is necessary to consider other turning operations and also different machining operations such as boring, drilling and milling. Grinding will be examined in Chap. 5.

For facing on a lathe, the onset of chatter was governed by the width of cut. This width was the length of the cutting edge in contact with the work, and it was perpendicular to the direction that most affected the chip thickness, i.e. the feed direction, see Fig. 2.12a. The question to be answered is does this apply to all machining operations?

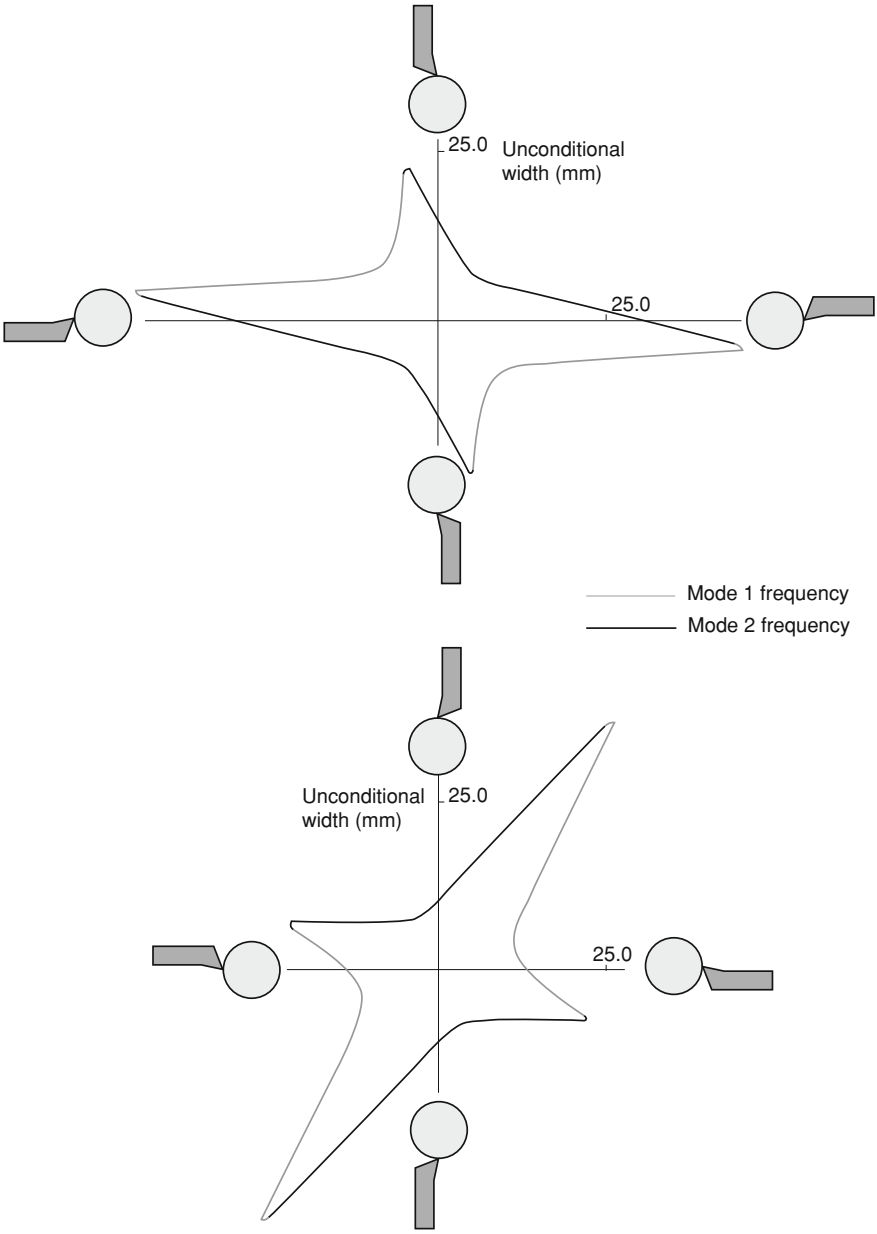

Fig. 2.11 Variation of unconditional width with circumferential position for inverted and conventional tool mounting (Program 2.6)

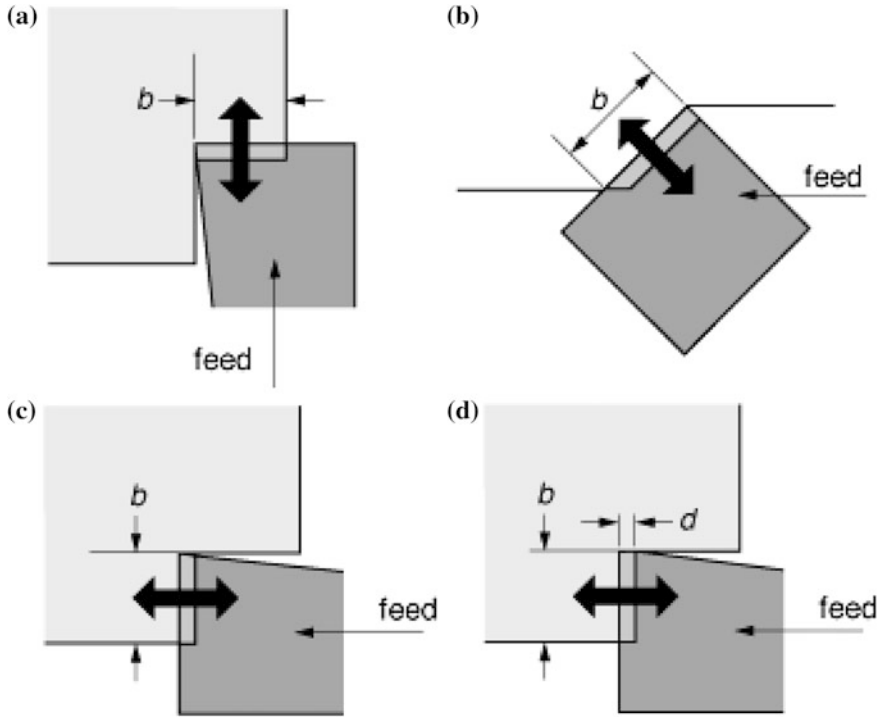

Fig. 2.12 The width of cut for various turning operations

2.5.1 Turning

If the case of parallel turning is considered, see Fig. 2.12b, the chip cross section is as shown. For the chatter model that has been developed, the variation in oscillating force depends in the first place on the varying area of this chip. The width of the chip is still the contact length of the cutting edge with the work. However, the direction (x) that most affects the chip thickness is not the feed direction. It is, however, perpendicular to the cutting edge and the cut surface. Thus, facing and parting off, which have the chip thickness direction the same as the feed direction, do not represent all machining operations. Also, for facing, the cutting force was considered to act in a plane that was perpendicular to the cutting edge. The direction was assumed to be at an angle β to the chip thickness direction. For parallel turning, the direction of the cutting force is assumed to be subject to the same rules. Thus, to begin to generalise,

1. The width of cut is the length of the cutting edge in contact with the work.
2. The chip thickness direction (x) is perpendicular to the cutting edge and the cut surface.

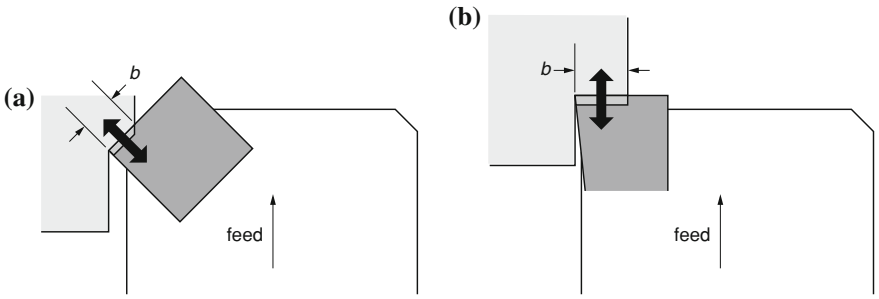

Fig. 2.13 The width of cut for boring

3. The cutting force is taken to act on an angle β to the chip thickness direction and in a plane perpendicular to the cutting edge.
4. The chatter receptance is the ratio of the response in the x direction to a force in the cutting force direction.

For parallel turning, it is important to note that the mode(s) of vibration that cause chatter are usually in a plane perpendicular to the spindle axis. As noted in Sect. 2.3, if the mode direction is perpendicular to either the x direction or force direction, the likelihood of chatter is greatly reduced. With the appropriate tool, it is possible in parallel turning to make the x direction perpendicular to the spindle axis, see Fig. 2.12c, with the expectation of improved chatter performance. This is found experimentally to be the case. However, if the tool has a sharp corner as shown, a spiral "thread" will be left on the cut surface. This may be overcome by using a tool shaped as in Fig. 2.12d. However, if the dimension d is too large, then vibration (and chatter) may occur in a direction perpendicular to the spindle axis.

2.5.2 Boring

Boring has great similarities to parallel turning. Figure 2.13a shows the width of cut and chip cross section for a typical operation. The width of the chip is the contact length of the cutting edge with the work, and the direction (x) that most affects the chip thickness is perpendicular to the cutting edge. Thus, boring may be considered as internal turning.

In practice, it is found that chatter is very common with long boring bars. This is because they have very little damping and easily vibrate in a transverse direction, i.e. perpendicular to their axes. Thus, it can be helpful to ensure that the chip width is perpendicular to the preferred vibration direction as shown in Fig. 2.13b. Methods of increasing the damping of boring bars will be considered further in Chap. 4.

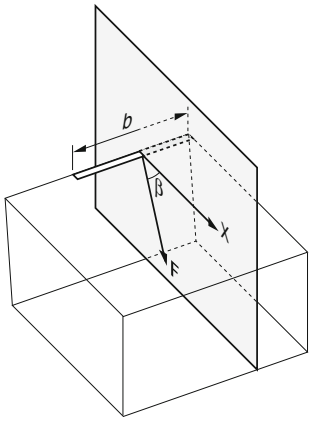

Fig. 2.14 Force and displacement directions for turning or boring

At this stage, it is possible to show the x direction and the force direction for any turning or boring operation, see Fig. 2.14. The x and F directions do not depend on the feed direction.

The cutting edge has so far been considered only to feed in a straight line, whether radial or axially. It is now necessary to consider what happens when the cutting edge is rotating as in drilling.

2.5.3 Drilling

For turning and boring, the cutting edge moved, but its orientation did not change, and the cutting edge did not rotate. In drilling, the complexity of chatter theory is now increased as there are two cutting edges and they are rotating and inclined to each other. Figure 2.15 shows, for each cutting edge, the chip cross sections. The x and F directions for each chip are also shown using the information from Fig. 2.14. The combination of the two forces produces a resultant force that acts along the axis of the drill. The question to be answered is "What is the direction of vibration that will most likely cause chatter by producing a variation in the chip thickness?" Transverse vibration of the drill (perpendicular to the feed) may be a problem on entry, but once drilling is in process, it is not normally a problem. An axial vibration will cause a variation of the same amount in both chips. It follows that chatter may occur in the axial direction of the drill. In this case, the effective total width, perpendicular to the direction affecting the chip thickness, is the diameter of the drill, see Fig. 2.16a.

The governing chatter receptance for drilling is thus the axial response resulting from an axial force. It is appropriate to restate that this receptance is that resulting from equal and opposite forces on drill and work and the response is the relative axial displacement between drill and work. Some of the earliest work on regenerative chatter was on radial arm drilling machines [4]. The theory developed previously is

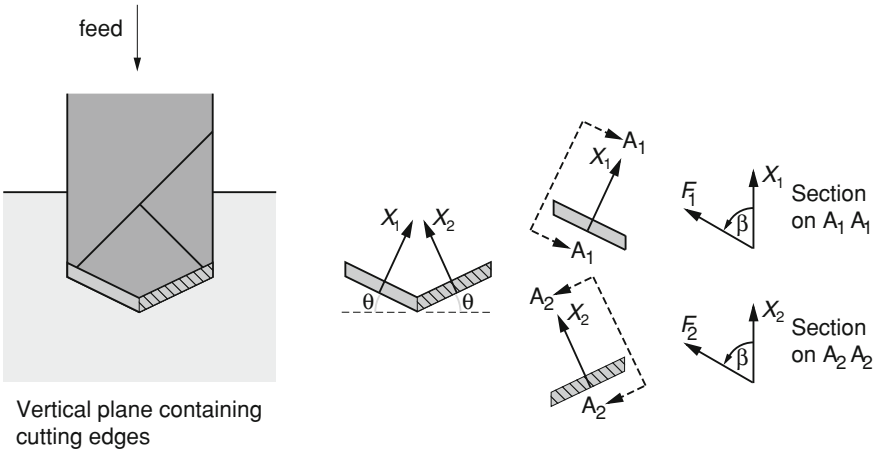

Fig. 2.15 Chip cross sections and forces for drilling

applicable with the value of b representing the diameter of the drill, but with one major change. For turning and boring, the time before a surface wave is cut again (τ) was the time for one revolution of the work. For drilling, it is the time between the two cutting edges. This is half the time for one revolution of the drill ($\tau/2$). As a result, Eq. 1.21 expressing the phase between the regenerative and non-regenerative components of the force in turning/boring is modified for drilling to

$$\omega\tau/2 = 3\pi - 2\alpha + 2n\pi \tag{2.3}$$

Hence, if the chatter receptance was the same, the stability lobes will occur at half the speed compared to turning/boring. However, the unconditional width of cut (i.e. drill diameter) is not affected—only the location of the stability lobes along the speed axis.

2.5.3.1 Enlarging Holes/Spot Facing

It is often the case when drilling that a hole is being enlarged (see Fig. 2.16b). In this case, the total width of cut b is the difference between the diameters of the drill and the existing hole.

Spot facing is very similar to drilling but with the angle θ in Fig. 2.15 zero. However, spot facing cutters often have four teeth resulting in a total width of cut b that is four times the width of cut for one tooth. Also the time between teeth is one quarter of the time for one revolution. Thus, Eq. 2.3 becomes

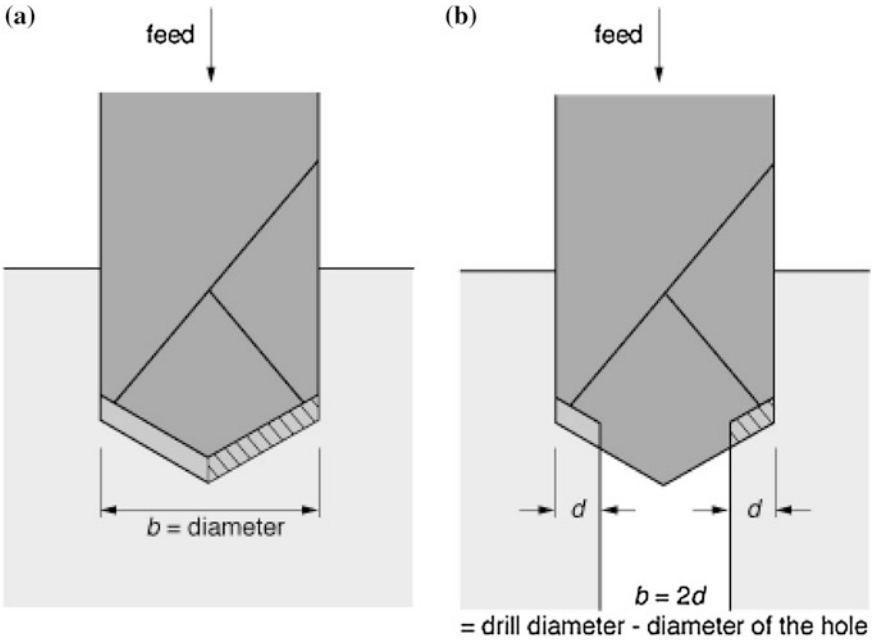

Fig. 2.16 The effective width of cut for drilling

$$\omega\tau/4 = 3\pi - 2\alpha + 2n\pi \tag{2.4}$$

As a result, the stability lobes occur at one quarter of the speed compared to turning/boring. In summary, the speed at which a stability lobe resides is inversely proportional to the number of cutting edges on the rotating tool.

2.5.3.2 Torsional Vibration

It was noted above that the resultant force in drilling acted along the axis of the drill. However, the forces acting on the two cutting edges also produce a torque. The question therefore arises as to whether it is possible to have torsional chatter in drilling? For chatter to involve torsional vibration, some form of regeneration must occur. For purely torsional vibration, without axial vibration, there would be no force variation unless the cutting force depends on speed. While any torsional vibration would cause a variation in speed, it would cause no variation in force and hence no chatter.

The practical situation is far more complicated. The cutting force is more complex than the model that simply relates force to the chip cross-sectional area. Also it is possible for torsional vibration and the axial vibration to be coupled by a structural mode. Even when not so coupled, an axial vibration causes both an

oscillating force and an oscillating torque that will excite torsional vibration. Historically, torsional vibration has been ignored for drilling. The model that assumes only axial vibration has been found to be useful in solving chatter problems in drilling. Nevertheless, when chatter occurs, there may be associated and large torsional vibrations.

2.5.4 Milling

For turning, boring and drilling, the cutting edge was straight. However, for milling, the cutting edge is often part of a helix. As a result, the direction that affects chip thickness varies along the length of the cutting edge. Figure 2.17a shows the chip cross section for a typical helical tooth. If this chip is considered as a series of small-width chips, then the directions that affect chip thickness vary along the chip, as shown in Fig. 2.17a, and moreover, the cutting force direction also varies along the chip. For simple models of chatter in milling, it is conventional to use an average chip thickness direction, as shown in Fig. 2.17b, that bisects the arc of contact and passes through the axis of rotation, O, of the cutter. There is also an implicit assumption that the effective displacement and force direction are in a plane perpendicular to the axis of rotation of the cutter. However, the helix angle causes both the displacement and force to have components along the axis of rotation. Nevertheless, when looking for solutions to chatter in milling, these conventional assumptions have produced practical solutions.

In passing, it is important to note why a helix angle is employed on milling cutters. The width of contact with the work is often large, and a straight tooth would engage the full width at the same instant. This would give rise to large impacts on engagement and, when leaving the cut, exciting significant forced vibration in the drive train. The helix angle allows each tooth to gradually come into engagement and gradually leave the cut.

Returning to chatter, it is necessary to determine not only the effective displacement and force directions but also the effective width of cut. For practical reasons, the width of the work in contact with the cutter is defined as b, see Fig. 2.18. However, in the equations developed previously, b has been the length of the cutting edge in contact with the work. From Fig. 2.18, it may be seen that as the cutter rotates each cutting edge comes in contact with the arc of cut in such a way that the length in contact increases from zero to a maximum and then reduces to zero. For the example shown, the maximum length of contact remains constant for a short time. Also at any instant, more than one cutting edge may be in contact with the work. To use the theory developed previously, it is necessary to estimate an average length in contact. An approximation may be obtained by determining the average number of teeth in contact via the angle, θ, subtended by the arc of cut. From Fig. 2.18 $\cos\theta = \frac{R-d}{R}$, where R is the radius of the cutter and d the depth of cut.

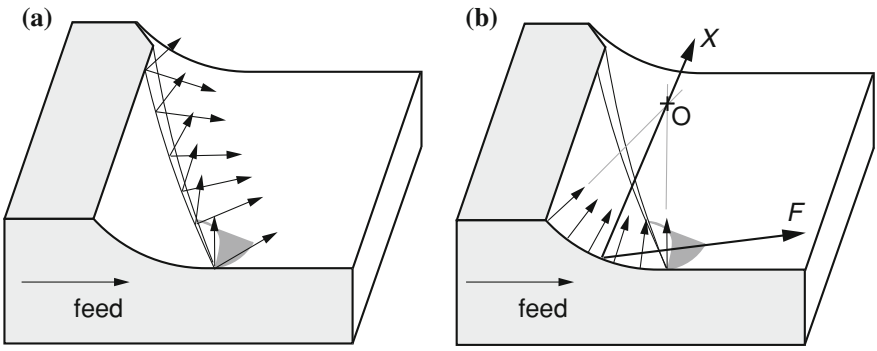

Fig. 2.17 Variation of displacement and force directions along a helical tooth

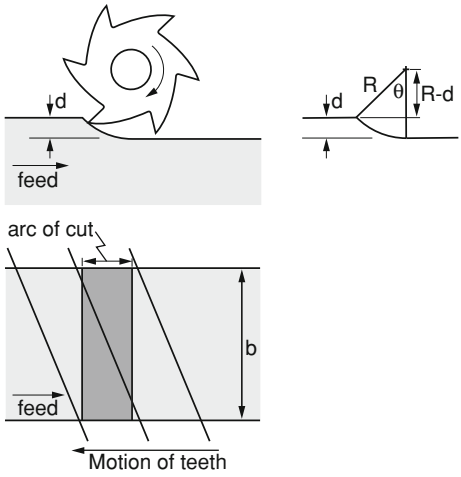

Fig. 2.18 Width of cut for milling

If there are N teeth on the cutter, the average number of teeth, z_c, in contact with the arc of cut will be $z_c = \frac{N\theta}{2\pi}$, where θ is in radians.

Thus, the average effective width in contact is $z_c b$ and substituting in Eq. 1.15 gives $z_c b = \frac{-1}{2RG_R(\omega)}$ so that at the stability boundary $b_{\lim} = \frac{-1}{2Rz_c\, G_R(\omega)}$.

And similarly substituting in Eq. 1.20 gives

$$b_{\lim} = \frac{1}{2Rz_c S\cos(180 - \alpha)} \tag{2.5}$$

Thus, the limiting work width, $b_{\lim}$, above which chatter may occur is modified by the reciprocal of z_c. Provided all of the assumptions made are reasonable, this means that $b_{\lim}$ is reduced by having a larger number of teeth on the cutter. z_c is also increased when the depth of cut is increased. However, the effect on the stable

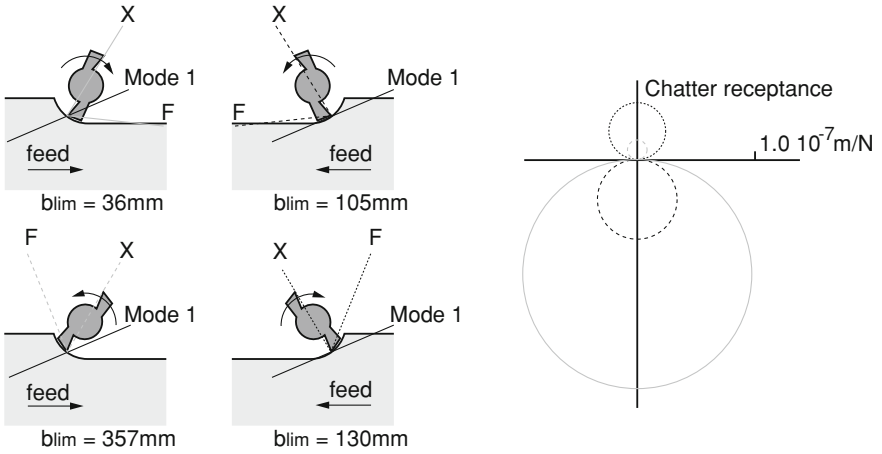

Fig. 2.19 Change in chatter receptance with machining configuration for a single mode, cutting depth 20 mm (Program 2.7)

width is then not immediately clear as changing the depth of cut will change the average directions of the displacement X and the force F. This in turn means that the mode directions are significant, as will be shown below. Milling operations may involve climb or conventional milling (as depicted in Figs. 2.19, 2.20, 2.21, 2.22) with consequential changes in the displacement and force directions, and this may have a significant effect on chatter.

Consider first a milling machine with one significant mode as shown in Fig. 2.19. The mode has $k = 4 \times 10^7$ N/m, $\omega_n = 100$ Hz, $\xi = 0.05$ and with the mode direction $\gamma = 20°$ to the horizontal. A two-tooth cutter was chosen to simplify the diagrams with a depth of cut $d = 20$ mm and a cutter radius of 30 mm. Four machining configurations are possible, and the chatter receptance for each is shown. The displacement direction, X, is normal to the arc of cut and the force at 60° to the displacement. For each configuration, the unconditional width of the work is shown for a cutting force coefficient $R = 4.0 \times 10^8$ N/m^2. Recall that there would be stability lobes on the associated stability charts. It is important to note that this simulation predicts a large improvement to be obtained by using the best configuration $b_{\text{lim}} = 357$ mm when climb milling feed left to right, compared to the worst, $b_{\text{lim}} = 36$ mm when conventional milling feed left to right.

The predicted variation in performance changes with the depth of cut. Figure 2.20 shows the variation when the depth of cut is increased to 50 mm, with all of the other variables remaining unchanged. Note that not only do the displacement and force directions change, but the average number of teeth in contact increases. For this case, the best configuration gives $b_{\text{lim}} = 74$ mm while climb milling feed right to left, and the worst gives $b_{\text{lim}} = 20$ mm while conventional milling feed right to left.

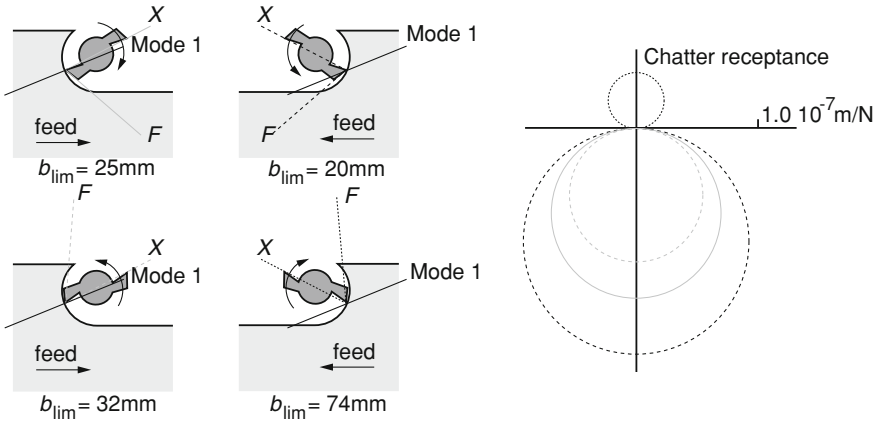

Fig. 2.20 Change in chatter receptance with machining configuration for a single mode, cutting depth 50 mm (Program 2.7)

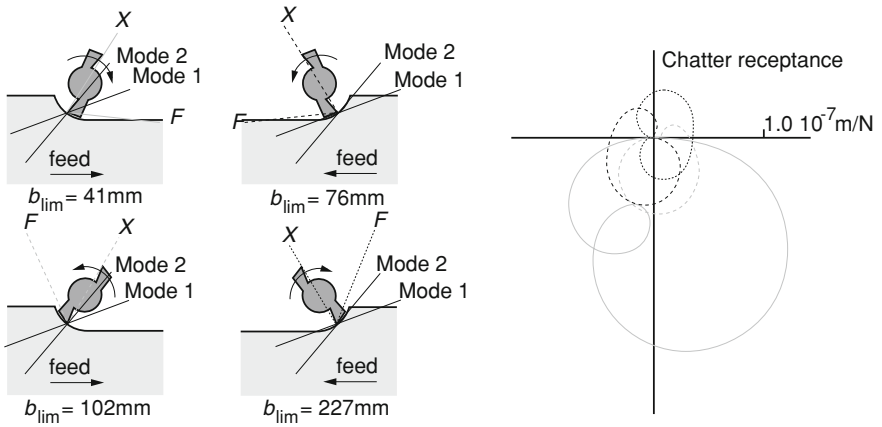

Fig. 2.21 Change in chatter receptance with machining configuration for two modes, cutting depth 20 mm (Program 2.8)

When there are several vibration modes with different directions, the situation is more involved. Figure 2.21 shows the comparative performance for a chatter receptance consisting of two modes with the following characteristics:

Mode 1: $k_1 = 4 \times 10^7$ N/m, $\omega_{n1} = 100$ Hz, $\xi_1 = 0.05$, mode direction $\gamma = 20^o$
Mode 2: $k_2 = 6 \times 10^7$ N/m, $\omega_{n2} = 120$ Hz, $\xi_2 = 0.05$, mode direction $\gamma = 50^o$

The other parameters are the same as those used to generate Fig. 2.19. For this situation, the best configuration gives $b_{\text{lim}} = 227$ mm while climb milling feed right to left and the worst gives $b_{\text{lim}} = 41$ mm while conventional milling feed left to right.

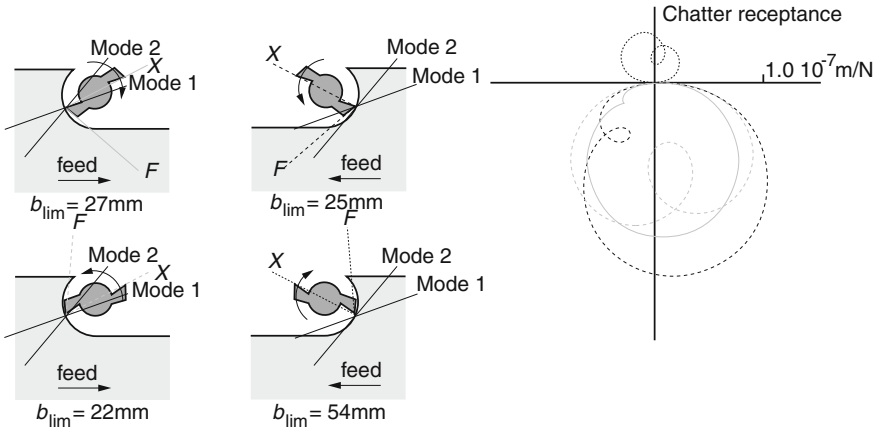

Fig. 2.22 Change in chatter receptance with machining configuration for two modes, cutting depth 50 mm (Program 2.8)

Figure 2.22 shows the result when the depth of cut is increased to 50 mm. For this situation, the best configuration gives $b_{\text{lim}} = 54$ mm while climb milling feed right to left and the worst gives $b_{\text{lim}} = 22$ mm while climb milling feed left to right.

For all of the examples given, it is important to note that when the number of teeth on the cutter is doubled to four, the predicted values of b_{lim} are halved.

It is concluded, and found to be the case in practice, that to improve chatter performance in milling, cutters should have the fewest teeth possible and choosing the best machining configuration (by experimenting) can lead to significant improvements.

It is appropriate to consider a stability chart including the stability lobes. For turning and boring, it was noted that the time before a surface wave is cut again (τ) was the time for one revolution of the work. For drilling, it was the time between the two cutting edges. For milling, the time before a surface wave is cut again is τ/N where N is the number of teeth and so, in general, the phase condition equation becomes

$$\omega\tau/N = 3\pi - 2\alpha + 2n\pi \tag{2.6}$$

Thus, the number of teeth on a cutter affects the unconditional stable width and also the location of the stability lobes along the speed axis of the stability chart. An example of a stability chart (without penetration rate damping) is shown in Fig. 2.23. The same parameter values were used as for Fig. 2.19 but for a cutter with four teeth. It is important to note that as the number of teeth is increased the last lobe occurs at a lower speed. This is significant for high-speed milling where machining may occur close to or above the last lobe.

The milling operation used for the examples given applies to slab milling or milling with an end mill. The operation known as face milling has some differences.

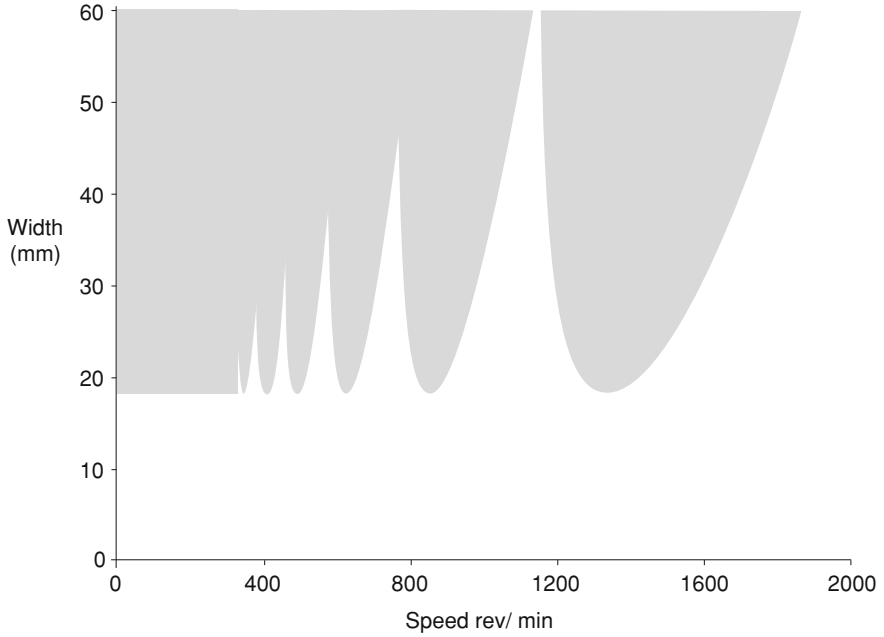

Fig. 2.23 Stability chart for milling with one significant mode (Program 2.9)

2.5.5 Face Milling

Figure 2.24 shows a typical face milling cutter. It is conventional for this application to determine the depth of cut (d) at the stability boundary. This depth is directly related to the width of the contact with each cutting edge, which is normally an insert. The motion of the inserts is directly analogous to that of the teeth during slab milling and end milling. Thus, there is an arc of cut and the average displacement direction and force direction are determined in the same way. The depth of cut, d, shown in Fig. 2.24, is here equivalent to the work width used above for slab milling.

If the width of the work while face milling is smaller than the cutter diameter as shown in Fig. 2.25, then there is the possibility of changing the directions of the average force and displacement relative to the mode directions of the machine. Figure 2.25 shows three possible machining configurations and the associated displacement and force directions. These three configurations show two extreme locations (a) and (c), where the cutter just overlaps the work. The configuration (b) is when the cutter is central to the work. Depending on the mode/s causing chatter and the mode directions, the three configurations may have significantly different stable depths of cut.

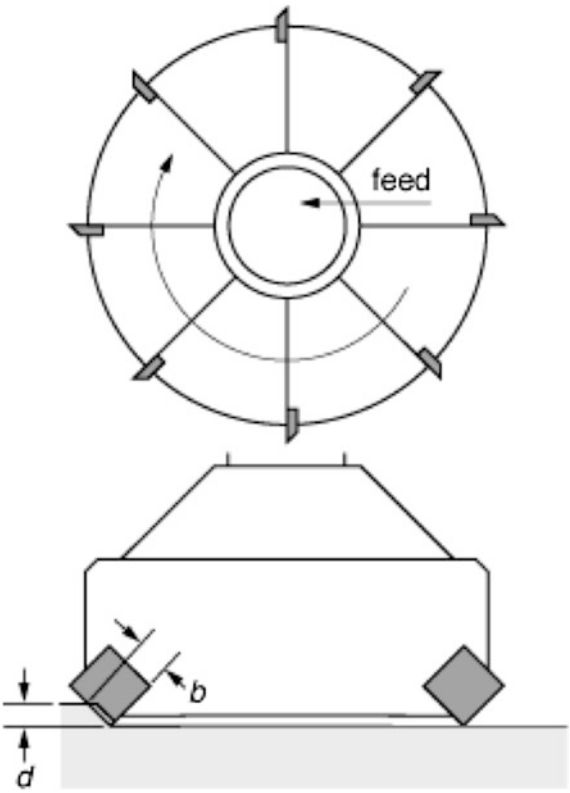

Fig. 2.24 Typical face milling cutter

2.6 Mode-Coupling Chatter

Now that multiple modes with associated mode directions have been considered, it is possible to describe another form of chatter. This is called mode-coupling chatter and occurs without any regeneration. For the machining operations considered thus far, the wave left by a cutting edge was subsequently cut by the same cutting edge or another tooth on the same tool. When turning a thread or turning with a large feed, any surface wave left by the cutting edge is not machined one revolution later, and so, there is no regeneration. Figure 2.26 shows this form of chatter when using a boring bar with a feed equal to the contact length of the tool. The feed/rev is the contact length b, and the depth of cut d.

Typically, boring bars have cross sections with different principal second moments of area that result in two vibration modes with mode directions at right angles. These modes may each be modelled as single-degree-of-freedom systems to illustrate this type of chatter. Figure 2.27 shows the orientation of the two modes relative to cutting edge.

For the simplified analysis that follows, it is assumed that the effective cutting speed of the work does not affect the force. Hence, the force is the cutting force

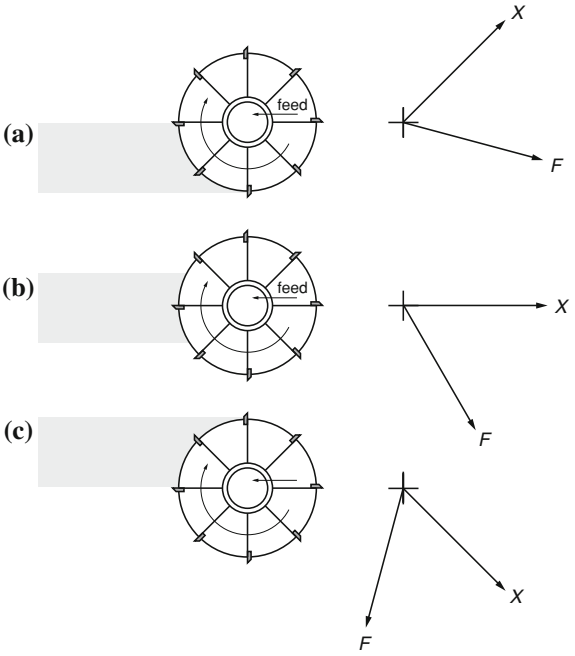

Fig. 2.25 Effect of position of face mill with respect to the work

coefficient (R) times the undeformed chip cross section (bd), i.e. Rbd. Let the cutting force act at an angle β from the horizontal as shown in Fig. 2.27.

Now, let Mode 1 be at an angle α from the horizontal. Then, for "thread cutting" with no overlap, i.e. no regeneration, for Mode 1, the equation of motion is

$$m_1 \frac{\mathrm{d}^2 x_1(t)}{\mathrm{d}t^2} + c_1 \frac{\mathrm{d}x_1(t)}{\mathrm{d}t} + k_1 x_1(t) = -Rb(x_1(t)\cos\alpha + x_2(t)\sin\alpha)\cos(\beta - \alpha), \tag{2.7}$$

and for Mode 2,

$$m_2 \frac{\mathrm{d}^2 x_2(t)}{\mathrm{d}t^2} + c_2 \frac{\mathrm{d}x_2(t)}{\mathrm{d}t} + k_2 x_2(t) = Rb(x_1(t)\cos\alpha + x_2(t)\sin\alpha)\sin(\beta - \alpha) \tag{2.8}$$

Assume solutions of the form $x_1(t) = A_1 \mathrm{e}^{(\sigma + \mathrm{i}\omega)t}$ and $x_2(t) = A_2 \mathrm{e}^{(\sigma t + \mathrm{i}[\omega t - \phi])}$ so that the motion is sinusoidal and growing exponentially. Substituting in Eqs. 2.7 and 2.8,

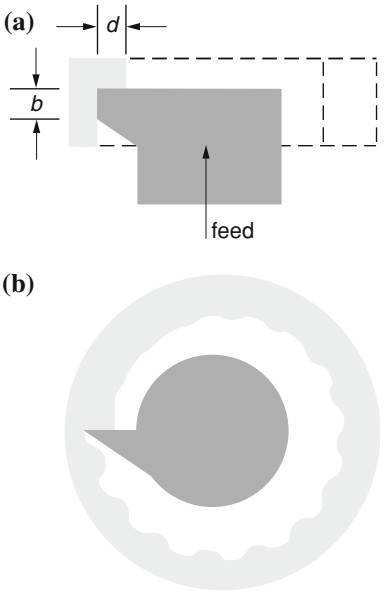

Fig. 2.26 Boring with no overlap

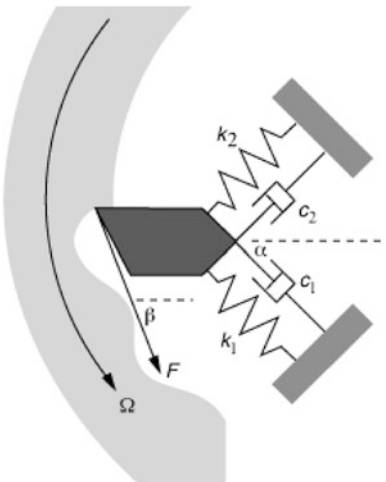

Fig. 2.27 Orientation of modes relative to the cutting position

$$m_1(\sigma+i\omega)^2 A_1 e^{(\sigma+i\omega)t} + c_1(\sigma+i\omega)A_1 e^{(\sigma+i\omega)t} + k_1 A_1 e^{(\sigma+i\omega)t} = -Rb\left(A_1 e^{(\sigma+i\omega)t}\cos\alpha + A_2 e^{(\sigma t+i[\omega t-\phi])}\sin\alpha\right)\cos(\beta-\alpha)$$

$$m_2(\sigma+i\omega)^2 A_2 e^{(\sigma t+i[\omega t-\phi])} + c_2(\sigma+i\omega)A_2 e^{(\sigma t+i[\omega t-\phi])} + k_2 A_2 e^{(\sigma t+i[\omega t-\phi])} = Rb\left(A_1 e^{(\sigma+i\omega)t}\cos\alpha + A_2 e^{(\sigma t+i[\omega t-\phi])}\sin\alpha\right)\sin(\beta-\alpha)$$

Expanding and dividing throughout by A_2, putting $A_1/A_2 = p$ and multiplying the second equation throughout by $e^{i\phi}$ gives

$$m_1(\sigma + i\omega)^2 p + c_1(\sigma + i\omega)p + k_1 p = -Rb\left(p\cos\alpha + e^{-i\phi}\sin\alpha\right)\cos(\beta - \alpha)$$
$$m_2(\sigma + i\omega)^2 + c_2(\sigma + i\omega) + k_2 = Rb\left(pe^{i\phi}\cos\alpha + \sin\alpha\right)\sin(\beta - \alpha)$$

Collecting real and imaginary parts of each equation,

$$m_1(\sigma^2 - \omega^2)p + c_1\sigma p + k_1 p = -Rb(p\cos\alpha + \cos\phi\sin\alpha)\cos(\beta - \alpha)$$
$$m_1 2\sigma\omega p + c_1\omega p = Rb\sin\phi\sin\alpha\cos(\beta - \alpha)$$
$$m_2(\sigma^2 - \omega^2) + c_2\sigma + k_2 = Rb(p\cos\phi\cos\alpha + \sin\alpha)\sin(\beta - \alpha)$$
$$m_2 2\sigma\omega + c_2\omega = Rbp\sin\phi\cos\alpha\sin(\beta - \alpha)$$

These represent four equations with four unknowns σ, ω, p and ϕ. To find the stability boundary, put $\sigma = 0$ with b as an unknown. Then,

$$\left(k_1 - m_1\omega^2\right)p = -Rb(p\cos\alpha + \cos\phi\sin\alpha)\cos(\beta - \alpha) \tag{2.9}$$

$$c_1\omega p = Rb\sin\phi\sin\alpha\cos(\beta - \alpha) \tag{2.10}$$

$$\left(k_2 - m_2\omega^2\right) = Rb(p\cos\phi\cos\alpha + \sin\alpha)\sin(\beta - \alpha) \tag{2.11}$$

$$c_2\omega = Rbp\sin\phi\cos\alpha\sin(\beta - \alpha) \tag{2.12}$$

Dividing Eq. 2.10 by Eq. 2.12 gives

$$\frac{\sin\alpha\cos(\beta - \alpha)}{p\cos\alpha\sin(\beta - \alpha)} = \frac{c_1\omega p}{c_2\omega}$$

and rearranging gives

$$p = \sqrt{\frac{c_2\sin\alpha\cos(\beta - \alpha)}{c_1\cos\alpha\sin(\beta - \alpha)}} \tag{2.13}$$

Divide Eq. 2.11 by Eq. 2.9

$$\frac{(p\cos\phi\cos\alpha + \sin\alpha)\sin(\beta - \alpha)}{-(p\cos\alpha + \cos\phi\sin\alpha)\cos(\beta - \alpha)} = \frac{(k_2 - m_2\omega^2)}{(k_1 - m_1\omega^2)p}$$

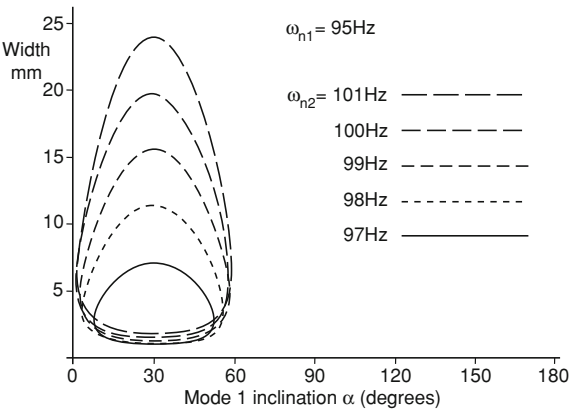

Fig. 2.28 Stability boundary for mode-coupling chatter (Program 2.10)

and rearranging to find cos ϕ

$$\cos\phi = -\frac{(k_1 - m_1\omega^2)p\sin\alpha\sin(\beta-\alpha) + (k_2 - m_2\omega^2)p\cos\alpha\cos(\beta-\alpha)}{((k_1 - m_1\omega^2)p^2\cos\alpha\sin(\beta-\alpha) + (k_2 - m_2\omega^2)\sin\alpha\cos(\beta-\alpha))} \tag{2.14}$$

Thus, we have p from Eq. 2.13 and for a given ω, we have ϕ from Eq. 2.14. From Eqs. 2.10 and 2.11, we can obtain two independent equations for b

$$b = \frac{c_1\omega p}{R\sin\phi\sin\alpha\cos(\beta-\alpha)}$$

$$b = \frac{(k_2 - m_2\omega^2)}{R(p\cos\phi\cos\alpha + \sin\alpha)\sin(\beta-\alpha)}$$

With a computer program, it is possible to search for value(s) of ω that give the same values of b from both equations. Figure 2.28 shows results for b against α for a boring bar with the following characteristics, $K_1 = 1.0 \times 10^7$ N/m, $\omega_{n1} = 95$ Hz, $\xi = 0.01$, cutting force direction $\beta = 60^o$.

The different curves are for different values of the second natural frequency ω_{n2}. It is assumed that the effective mass for each mode is the same as a boring bar is being considered. Thus, $\omega_{n1} = \sqrt{\frac{k_1}{m}}$ and $\omega_{n2} = \sqrt{\frac{k_2}{m}}$ so that eliminating m gives $k_2 = \frac{\omega_{n2}^2}{\omega_{n1}^2}k_1$.

The viscous damping ratio is considered to be the same for each mode so that $c_1 = 2\xi\sqrt{mk_1}$ and $c_2 = 2\xi\sqrt{mk_2}$.

It is found that mode-coupling chatter may only occur when the direction of the lower-frequency mode lies between the displacement and force directions. As shown in Fig. 2.28, there are, for any particular value of α in the required range,

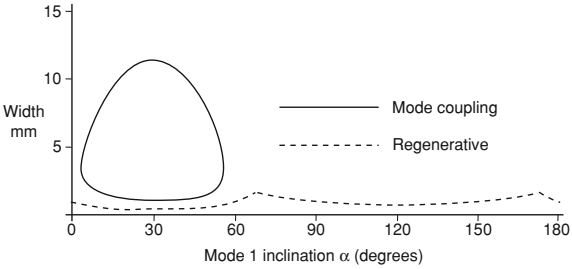

Fig. 2.29 Stability boundary for mode-coupling and regenerative chatter (Program 2.11)

normally two solutions for b. Instability occurs for values of b between these two values. Note that the solutions are independent of the rotational speed of the work.

The question arises as to how the limiting widths for mode-coupling chatter compare with those for regenerative chatter with the same structural model. Figure 2.29 shows a comparison for $k_1 = 1.0 \times 10^7$ N/m, $\omega_{n1} = 95$ Hz, $\omega_{n2} = 100$ Hz, $\xi = 0.01$ and the cutting force direction $\beta = 60^o$. The limiting width of cut for regenerative chatter is always significantly less than for mode-coupling chatter. For the model presented, mode-coupling chatter does not depend on speed. The boundary for regenerative chatter shown in Fig. 2.29 is the unconditional width.

Any particular machining operation can be much more complex than those chosen above to illustrate a single major effect. For example, in some machining operations, e.g. grinding (see Chap. 5), part of the surface wave regenerates but not the full width. Mode directions will not always be at right angles, as for the boring bar example above. Process damping will also have an effect when the surface waves have a short wavelength.

To illustrate the fact that mode-coupling chatter has a lower and upper stability boundary, a program (Program 2.12) was written that simulates boring. It is a time simulation of Eqs. 2.7 and 2.8. The simulation was written using a fourth-order Runge–Kutta approximation, and it is possible to vary the parameters and confirm that under certain conditions an increase in the width of cut will stop mode-coupling chatter. Using this animation, it will be found that when mode-coupling chatter occurs, the cutting edge moves anticlockwise around an ellipse. The consequence of this is that energy is input to the system and causes chatter.

2.7 Conclusions

The theory of regenerative chatter has been extended to a variety of machining operations, and several significant effects have been noted. In each case, assumptions were made so that the effect to be illustrated was highlighted. It is important to restate the assumptions that have been made and assess them.

- Regenerative chatter has been investigated assuming a constant-amplitude sinusoidal motion at the boundary of stability. In practice, no such state is normally achieved. However, experiments confirm that models of chatter based on this assumption reveal the major parameters governing chatter.
- The cutting force has been assumed to act in a fixed direction relative to the chip thickness direction. Many researchers have shown that the cutting force is more complex than this. However, again models of chatter based on the simple assumption do reveal the major parameters governing chatter.
- For milling cutters, the total length of all cutting edges in contact with the work varies with time as teeth enter and exit the arc of cut. Average values have therefore been assumed for both the displacement and the force directions. This assumption needs to be continuously borne in mind when considering solutions for chatter in milling.

This chapter has illustrated several methods that may usefully be employed to prevent chatter in addition to those presented in Chap. 1. Thus, the following solutions may be usefully employed.

- The total length of the cutting edge(s) in contact with the work should be reduced. For milling, this can be achieved by reducing the number of teeth on the cutter.
- The machining configuration should be chosen so that either the displacement or force direction is close to being perpendicular to the direction of the most significant mode.
- Machining between stability lobes may be possible. This is especially the case for high-speed milling when operating at a speed close to or above the last stability lobe.
- Process damping can be beneficial if the wavelength of chatter marks is small. This may be achieved by reducing the surface cutting speed.
- For mode-coupling chatter with a boring bar, chatter may be eliminated by ensuring that the direction of the lower-frequency mode does not lie between the displacement and force directions.

There is a considerable amount of literature on the topics covered in this chapter, a sample of which is given in the bibliography below. Many of these publications contain far more complex models of chatter, but it is found that the major parameters illustrated in this chapter remain the major ones affecting chatter.

Thus far, chatter theory has been developed to the stage where improvements can be made quite simply and experimentally. There are other ways of stopping chatter. In the next chapter, a range of chatter-resistant multi-tooth cutters will be presented and their performance assessed.

References

1. Gurney JP, Tobias SA (1961) A graphical method for the determination of the dynamic study of machine tools. Int J Mach Tool Des Res 1:148–156
2. Tlusty J, Polacek M (1968) Experience with analyzing stability of machine tool against chatter. In: Proceedings of 9th MTDR conference, vol 1, pp 521–570
3. Arnold RN (1946) The mechanism of tool vibration in the cutting of steel. Proc Inst Mech Eng 154(1):261–284
4. Tobias SA, Fishwick W (1956) The vibrations of radial drilling machines under test and working conditions. Proc Inst Mech Eng 170:232–247

Bibliography

Opitz H, Bernardi F (1969) Investigation and calculation of the chatter behaviour of lathes and milling machines. Annals of CIRP 18(1):335–343

Tlusty J (1986) Dynamics of high-speed milling. ASME J Eng Ind 108:509–687

Smith S, Tlusty J (1993) Efficient simulation programs for chatter in milling. Ann CIRP 42(1):463–466

Altintas Y, Budak E (1995) Analytical prediction of stability lobes in milling. Ann CIRP 44(1):357–362

Budak E, Altintas Y (1998) Analytical prediction of chatter stability in milling—part I: general formulation. J Dyn Sys Meas Control 120(1):22–30

Budak E, Altintas Y (1998) Analytical prediction of chatter stability in milling—part II: application of the general formulation to common milling systems. J Dyn Sys Meas Control 120(1):31–36

Altintas Y, Shamoto E, Lee P, Budak E (1999) Analytical prediction of stability lobes in ball end milling. Trans ASME J Manufact Sci Eng 121:586–592

Insperger T, Stepan G (2000) Stability of the milling process. Periodica Polytech Mech Eng 44(1):47–57

Li Z, Li XP (2000) Modelling and simulation of chatter in milling using predictive force model. J Mach Tools Manuf 40(14):2047–2071

Altintas Y (2001) Analytical prediction of three dimensional chatter stability in milling. Jpn Soc Mech Eng Int 44(3):717–723

Gasparetto A (2001) Eigenvalue analysis of mode-coupling chatter for machine-tool stabilization. J Vib Control 7(2):181–197

Altintas Y, Weck M (2004) Chatter stability in metal cutting and grinding. Ann CIRP 53(2):619–642

Merdol D, Altintas Y (2004) Multi frequency solution of chatter stability for low immersion milling. Trans ASME J Manufact Sci Eng 126(3):459–466

Li H, Shin YC (2006) Comprehensive dynamic end milling simulation model. ASME J Manuf Sci Eng 128(1):86–95

Altintas Y, Stepan G, Merdol D, Dombovari Z (2008) Chatter stability of milling in frequency and discrete time domain. CIRP J Manufact Sci Technol 1:35–44

Khachan S, Ismail F (2009) Machining chatter simulation in multi-axis milling using graphical method. Int J Mach Tools Manuf 49:163–170

http://www.springer.com/978-3-319-05235-9

Chatter and Machine Tools

Stone, B.

2014, XVI, 260 p. 209 illus. With online files/update.,
Hardcover
ISBN: 978-3-319-05235-9